Results in Engineering 24 (2024) 103419

Contents lists available at ScienceDirect

Results in Engineering

journal homepage: www.sciencedirect.com/journal/results-in-engineering

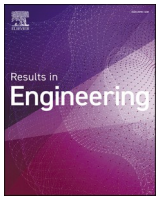

Enhancing laser surface texturing with driving training-based optimization: A metaheuristic approach

Ishwer Shivakoti [a,b], Sunny Diyaley [a], Partha Protim Das [a], Abhijit Bhowmik [c,d], A. Johnson Santhosh [e,*]

[a] Department of Mechanical Engineering, Sikkim Manipal Institute of Technology, Sikkim Manipal University, Sikkim, India
[b] Centre for Distance and Online Education, Sikkim Manipal University, Sikkim, India
[c] Department of Mechanical Engineering, Dream Institute of Technology, Kolkata 700104, India
[d] Centre for Research Impact & Outcome, Chitkara University Institute of Engineering and Technology, Chitkara University, Rajpura, Punjab 140401, India
[e] Faculty of Mechanical Engineering, Jimma Institute of Technology, Jimma University, Jimma, Ethiopia

ARTICLE INFO

Keywords:
DTBO algorithm
Laser surface texturing
Metaheuristic algorithms
Optimization

ABSTRACT

This paper investigates the capability of Laser Surface Textruing (LST) to induce texture on Ti-6Al-4V, aiming on optimizing process parameters viz. average power, pulse frequency, scanning speed, and gas pressure using the Driving Training-based Optimization (DTBO) algorithm. Both single and multi-objective optimizations are conducted to determine optimal parametric settings. The study systematically examines the impression of these LBM process parameters on various responses. Comparative analyses was performed with five other metaheuristic algorithms such as Ant colony optimization, Particle swarm optimization, Differential evolution, Firefly algorithm, Teaching-learning-based optimization, and Artificial bee colony. Furthermore, statistical validation via paired *t*-tests confirms the unique effectiveness of the DTBO algorithm. Detailed examination through developed box plots and convergence diagrams consistently demonstrates DTBO superior performance in terms of accuracy, minimal variability in optimal solutions, and reduced computational effort. The DTBO achieves a higher MRR by 35.7 %, 20 %, 11.9 %, 54.7 %, and 33.3 % compared to ABC, ACO, FA, DE, and TLBO, respectively. Simultaneously, DTBO also achieves a lower ATW by 13.6 %, 14.8 %, 3.02 %, 15.9 %, and 16.1 % compared to the same algorithms. These results underscore DTBO's superior performance in achieving improved MRR values and reduced ATW values across the considered optimization algorithms. Hence, The DTBO algorithm demonstrates robustness and applicability in optimizing LBM processes in context of laser texturing, which may enhance manufacturing efficiency and product quality significantly.

1. Introduction

Laser surface texturing (LST) has gaining widespread adoption among researchers across the globe. LST is preferred over other surface modification techniques based on its remarkable efficiency, exceptional controllability, accuracy and environmental friendly [1,2]. It creates micro/nanoscale surface structures on the surface of the materials offering non-toxic and non-polluting machining environment, with remarkable efficiency [3]. LST has been utilised effectively in several advanced materials such as polymers [4,5], ceramics [6,7] and metals [8,9]. The LST process parameters has a significant role in achieving high quality texture which progress the overall productivity of the process. Optimizing the process parameters of laser surface texturing (LST) plays a crucial role in attaining high-quality textures and enhancing process efficiency. Multi criteria decision making methods [10,11] and other optimization techniques have been used by researchers to determine the best possible parametric combinations during laser surface texturing. However, in recent years, material processing has witnessed the integration of metaheuristic algorithms [12,13], machine learning techniques [14–16], and hybrid approaches to optimize laser process parameters.

Metaheuristic-based optimization stands out as a robust method for addressing challenging optimization problems, offering acceptable solutions within a reasonable timeframe [17]. Ant colony optimization [18,19], Particle swarm optimization [20–22], Differential evolution [23,24], Firefly algorithm [25,26] and Teaching-learning-based

* Corresponding author.
E-mail address: johnson.antony@ju.edu.et (A.J. Santhosh).

https://doi.org/10.1016/j.rineng.2024.103419
Received 2 October 2024; Received in revised form 28 October 2024; Accepted 13 November 2024
Available online 14 November 2024

optimization [27,28] and Artificial bee colony optimization [29,30] techniques are some of the widely used metaheuristic optimization techniques by various researchers. However, very limited research has been done in laser surface texturing for determining optimal parametric combinations using metaheuristic algorithms, but was successfully implemented in other processes. Amongst, all a recently established Driving Training-Based Optimization (DTBO) technique has not been used in machining processes for determining the optimal parametric combinations, especially for laser surface texturing. The core concept of DTBO draws inspiration from the progression of erudition to drive, akin to attending driving school and tutor training. In comparative analyses against ten established algorithms, DTBO showcased superior performance, outperforming its counterparts [31].

In present work, an innovative stochastic metaheuristic optimization algorithm is utilised with the aim to minimize average texture width (ATW) and to maximize material removal rate (MRR) during laser surface texturing of Ti-6Al-4V. The problem is compounded by the fact that the LST process parameters (e.g., average power, pulse frequency, and scanning speed) are subject to real-time machining constraints and these parameters such as Average power, pulse frequency, scanning speed etc., if not precisely controlled, can lead to inaccurate textures and thereby reduced machining efficiency. The mentioned constraints are addressed in this paper using Driving Training-Based Optimization (DTBO) technique. However, to corroborate the performance of the DTBO the outcomes were compared with additional metaheuristic algorithms such as particle swarm optimization (PSO), artificial bee colony (ABC) optimization, teaching-learning-based optimization (TLBO), ant colony optimization (ACO), differential evolution (DE), firefly algorithm (FA), techniques.

2. Driving training-based optimization (DTBO)

The essence of Driving Training-Based Optimization (DTBO) [31] technique lies in its emulation of human driving training activities. Drawing inspiration from the structured learning process of typical driving schools and the guidance provided by instructors, DTBO is meticulously designed to reflect these elements. Learning to drive is a systematic procedure wherein a beginner undergoes training to develop driving proficiency. While enrolling in a driving school, a new beginner gets the option to select from a number of instructors. These instructors then impart the necessary instructions and techniques to the learner. The novice attempts to grasp driving skills under the supervision of the instructor and aims to apply them while driving. Moreover, regular personal practice also plays a critical role in further enhancing learner's driving abilities. It is mathematically conceptualized through three distinct phases: (1) initial training under the supervision of an instructor, (2) shaping student behavior through proper guidance based on instructor expertise, and (3) iterative practice sessions. This ground-breaking method leads towards development of a unique metaheuristic algorithm designed specifically to deal with optimization obstacles. The steps are as follows [31]:

The initial phase of DTBO is to develop a matrix formulated based on the population, wherein individuals represent both driving learners and instructors. These individuals, serving as applicant solutions for the optimization problem at hand, are organized within a matrix referred to as the populace matrix, as shown in Eq. (1). The starting positions at the beginning of implementation are erratically set applying Eq. (2).

$$A = \begin{bmatrix} A_1 \\ \vdots \\ A_i \\ \vdots \\ A_n \end{bmatrix}_{n\times m} = \begin{bmatrix} a_{11} & \cdots & a_{1j} & \cdots & a_{1m} \\ \vdots & \ddots & \vdots & \ddots & \vdots \\ a_{i1} & \cdots & a_{ij} & \cdots & a_{im} \\ \vdots & \ddots & \vdots & \ddots & \vdots \\ a_{n1} & \cdots & a_{nj} & \cdots & a_{nm} \end{bmatrix}_{n\times m} \tag{1}$$

$$a_{i,j} = l_j + t\cdot(l_j - u_j),\ i = 1,\ 2, \ldots..,n;\ j = 1,\ 2, \ldots..m \tag{2}$$

where A represents the population of DTBO, A_i depicts the i^{th} result, a_{ij} represents the valuation of j^{th} candidate obtained from i^{th} solution, n and m denotes the population size and count of problem variables respectively, t indicates a arbitrary number from the range [0, 1], l_j and u_j denotes the inferior and superior limits of the j^{th} problem variable correspondingly. Every potential result appoints values to the variables of the problem, are further validated based on the objective function. Subsequently, objective function value is calculated for each potential solution. Eq. (3) represents the vector encapsulating these objective function values.

$$P = \begin{bmatrix} P_1 \\ \vdots \\ P_i \\ \vdots \\ P_n \end{bmatrix}_{n\times 1} = \begin{bmatrix} P(A_1) \\ \vdots \\ P(A_i) \\ \vdots \\ P(A_n) \end{bmatrix}_{n\times 1} \tag{3}$$

where the vector P signifies the objective functions and P_i represents its value delivered by the i^{th} solution. The objective function values serve as the primary criteria for evaluating the quality of candidate solutions. Through comparing these objective function values, the member exhibiting the most favourable value is identified as the best member of the population (denoted as A_{best}). This best member must undergo updates alongside any enhancements in candidate solutions after each iteration.

In DTBO, candidate solutions undergo updates across three distinct stages: (i) driving instructor instructing the learner driver, (ii) modelling the learner's behaviour based on instructor skills, and (iii) the learner's practice sessions.

Stage 1: Instructor-guided Training (Exploration): In the initial phase of DTBO, the learner driver selects a driving instructor and receives training from them. Within the DTBO population, the top-performing members are designated as driving instructors, while the remaining members act as learner drivers. This selection process and skill acquisition encourage the population members to explore various regions within the search space. Such diversification enhances DTBO's global search capabilities, aiding in the discovery of optimal areas. Thus, this phase demonstrates the algorithm's exploratory strength. In each iteration, the top n members of DTBO are chosen as driving instructors, as outlined in Eq. (4).

$$D = \begin{bmatrix} D_1 \\ \vdots \\ D_i \\ \vdots \\ D_{n_D} \end{bmatrix}_{n_D\times m} = \begin{bmatrix} D_{11} & \cdots & D_{1j} & \cdots & D_{1m} \\ \vdots & \ddots & \vdots & \ddots & \vdots \\ D_{i1} & \cdots & D_{ij} & \cdots & D_{im} \\ \vdots & \ddots & \vdots & \ddots & \vdots \\ D_{n_D 1} & \cdots & D_{n_D j} & \cdots & D_{n_D m} \end{bmatrix}_{n_D\times m} \tag{4}$$

where D represents the driving instructors matrix, where D_i refers to the i^{th} instructor, and $D_{i,j}$ represents the j^{th} criterion within that instructor's skillset. The amount of instructors, denoted as n_D, is calculated as [$0.1 \times n \times (1 - t/T)$], where t represents the current iteration and T represents the maximum number of iterations.

The mathematical modelling of DTBO phase begins with the calculation of the latest location for each member applying Eq. (5). Subsequently, as per Eq. (6), this latest location supersedes the previous one if it enhances the objective function value.

$$a_{i,j}^{P1} = \begin{cases} a_{i,j} + s.\left(D_{k_i,j} - R.a_{i,j}\right), & F_{D_{k_i}} < F_i; \\ a_{i,j} + s.\left(a_{i,j} - D_{k_i,j}\right), & otherwise, \end{cases} \tag{5}$$

$$A_i = \begin{cases} A_i^{P1}, & F_i^{P1} < F_i; \\ A_i, & otherwise, \end{cases} \tag{6}$$

in this formulation, A_i^{P1} represents the newly calculated position for the i^{th} candidate solution, derived from the first phase of DTBO. $a_{i,j}^{P1}$ denotes its j^{th} dimension, and F_i^{P1} corresponds to its objective function value. The variable R is randomly chosen from the set {1, 2}, while s represents a

random number within the interval [0, 1]. Furthermore, $D_{k_i,j}$, where k_i is elected arbitrarily from the set {1, 2, …, n_D} and signifies an arbitrarily chosen driving instructor to teach the i^{th} member. $D_{k_i,j}$ represents its j^{th} criterion, and $F_{D_{k_i}}$ indicates its objective function value.

Stage 2: Emulation of Student Driver's Instructor Skills (Exploration): The next stage of the DTBO involves the learner driver emulating the actions of the instructor. In this phase, the learner endeavours to replicate all the actions and abilities demonstrated by the instructor. It prompts DTBO members to traverse diverse positions within the search space, thereby enhancing the exploration capacity of DTBO. To represent this concept mathematically, a fresh position is generated by combining linearly each member's position with that of the instructor, as described in Eq. (7). If this newly derived position leads to an improvement in the objective function's value, it supersedes the previous position as outlined in Eq. (8).

$$a_{i,j}^{P2} = P.a_{i,j} + (1-P).D_{k_i,j}, \tag{7}$$

$$A_i = \begin{cases} A_i^{P2}, & F_i^{P2} < F_i; \\ A_i, & otherwise, \end{cases} \tag{8}$$

where A_i^{P2} represents the newly calculated status for the i^{th} candidate solution based on the second phase of DTBO, $a_{i,j}^{P2}$ denotes its j^{th} dimension, F_i^{P2} represents its value of objective function, and P stands for the patterning index provided by

$$P = 0.01 + 0.9\left(1 + \frac{t}{T}\right) \tag{9}$$

The last stage of the DTBO emphasizes the personal effort of each learner to hone and improve their driving expertise. During this phase, each learner driver works diligently to achieve the highest possible level of optimization in their abilities. It involves a process where each member explores improvements within their current skill set, demonstrating the effectiveness of DTBO in exploiting local search capabilities. This phase is arithmetically formulated, beginning with the generation of a random position near each population member as per Eq. (10). Subsequently, based on Eq. (11), the new position substitutes the former one if it leads to an enhancement in the objective function's value.

$$a_{i,j}^{P3} = a_{i,j} + (1-2s).I.\left(1 - \frac{t}{T}\right).a_{i,j}, \tag{10}$$

$$A_i = \begin{cases} A_i^{P3}, & F_i^{P3} < F_i; \\ A_i, & otherwise, \end{cases} \tag{11}$$

where, A_i^{P3} is the newly computed location for the i^{th} solution, derived after the third phase of DTBO. $a_{i,j}^{P3}$ updates the j^{th} dimension of the solution, $F_i^{P3}$is the objective function value obtained considering a random real number s from the interval [0, 1]. I is a constant, set to 0.05, while t represents the current iteration and T stands for the maximum iterations.

Once the population members have been updated through the first three phases, a single iteration of the DTBO is completed. The algorithm then proceeds to the next iteration with the updated population. This iterative process repeats the steps from the first to the third phases, following Eqs. (4) to (11), until the maximum number of iterations is reached. Upon completing the DTBO implementation on the given problem, the most optimal candidate solution identified during the process is designated as the final solution. The pseudocode for the proposed DTBO method is shown in Algorithm 1, and its corresponding flowchart is illustrated in Fig. 1.

3. Experimental details

The experimental data utilised in this present study was conducted by [32], the experiments were conducted on Ti-6-Al-4V material, utilising Multi-diode Nd: YAG laser taking average power, pulse frequency, scanning speed and gas pressure as laser texturing variables. The horizontal micro grooves were created, constituting a desired texture. The MRR and ATW was measured and considered as performance criteria. The experimental data has been utilised to formulate mathematical relationship using regression analysis. The second order quadratic equation obtained through regression analysis has been used for optimization using Driving Training-Based Optimization (DTBO) technique. Furthermore, the identical equation underwent optimization through a spectrum of metaheuristic algorithms such as Ant colony optimization, Particle swarm optimization, Differential evolution, Firefly algorithm, Teaching-learning-based optimization, and Artificial bee colony optimization. However, the focal point of the paper lies in the thorough exploration of DTBO, given its novelty in machining processes. By extensively comparing DTBO with the algorithms, the study provides insights on its efficacy and potential in optimizing laser texturing parameters for Ti-6-Al-4V material. This comprehensive analysis not only enhances understanding of machining optimization but also emphasizes

Algorithm 1
DTBO Optimization.

1. **Input**: Obtain details of the optimization problem.
2. **Initialization**:
   - o Set n to represent the population size.
   - o Set T to represent the maximum number of iterations.
   - o Initialize the positions of the DTBO population.
   - o Evaluate the objective function for the initial population.
3. Iterative Optimization Process:
   - o For each iteration t from 1 to T:
   - o For each individual i in the population of size n:
     - • Phase 1: Exploration by Driving Instructor:
       Compare objective function values to form the driving instructor matrix D.
       Randomly choose an instructor from this matrix.
       Compute the new position for individual i.
       Update the position of individual i.
     - • Phase 2: Exploration via Learner Driver Patterning:
       Calculate the patterning index P.
       Determine the new position of individual i.
       Update the position of individual i.
     - • Phase 3: Exploitation through Personal Practice:
       Compute the new position for individual i.
       Update the position of individual i.
       Update the best candidate solution found so far.
4. **Output**: Present the best candidate solution identified by the DTBO algorithm.

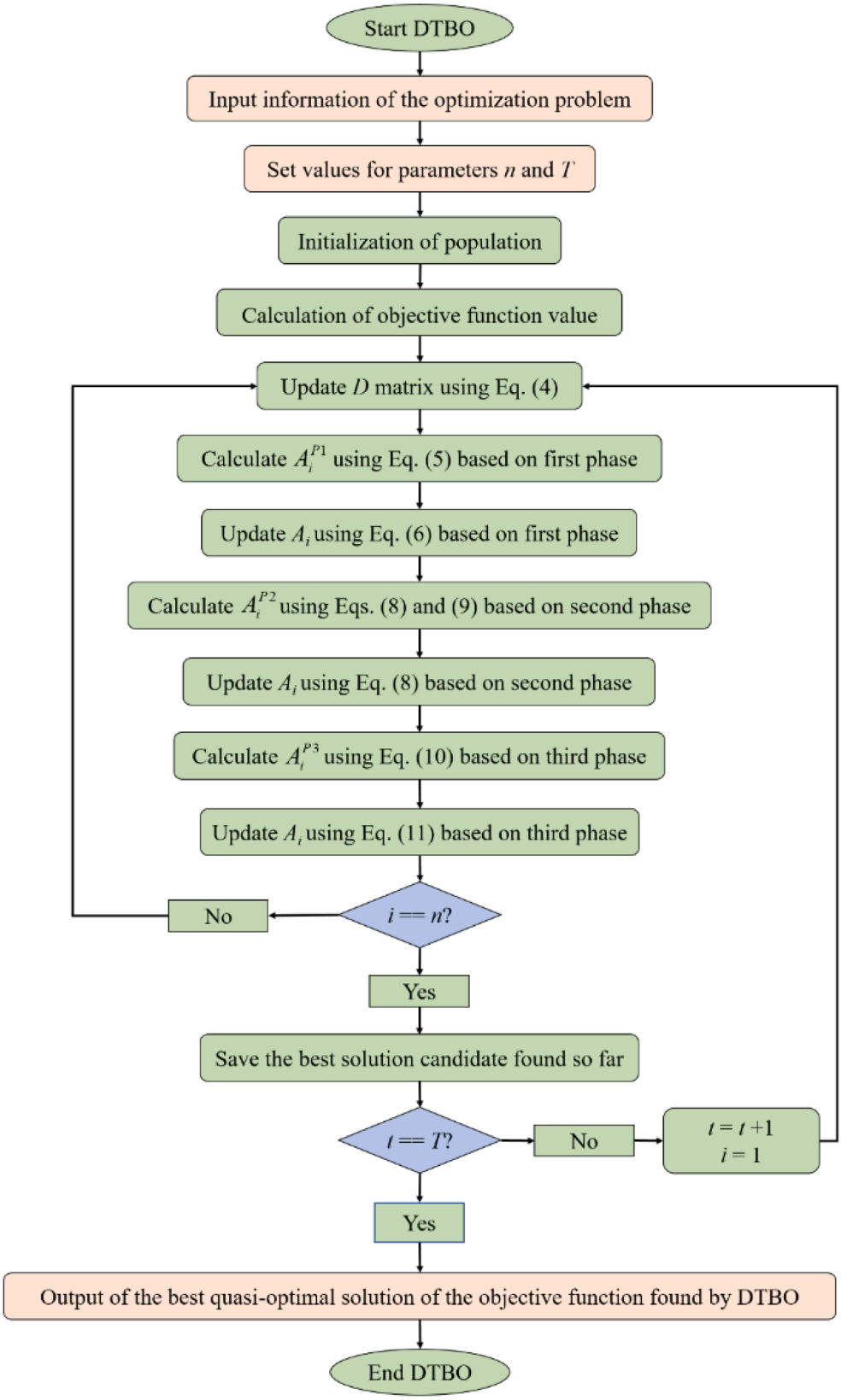

Fig. 1. Flowchart of DTBO.

the significance of DTBO as a promising tool in this domain.

4. Optimization of the LBM process

The experimental data [32] and applying Minitab software (R17), the mathematical relationship based on regression equation are established for both MRR and ATW, respectively. In the established equations, second order and its interaction effect amongst the laser beam process variables were considered. It was also observed that the developed equations had greater values of coefficient of determination (R^2) indicating the relationship amongst the responses and process parameters, which proves that these equations are the best fit models.

$$MRR = -0.0011 + 0.000459x_1 - 0.000211x_2 + 0.000158x_3 + 0.00380x_4 - 0.000005{x_1}^2 + 0.000002{x_2}^2 - 0.000003{x_3}^2 - 0.00142{x_4}^2 \quad (12)$$

$$ATW = -6.8 - 0.240x_1 + 0.346x_2 + 0.087x_3 + 0.73x_4 + 0.0077{x_1}^2 - 0.00261{x_2}^2 - 0.00174{x_3}^2 - 0.34{x_4}^2 \quad (13)$$

To elucidate this problem by applying the mentioned algorithms for single and multi-objective criteria for laser surface texturing, the developed equations are solved with constraints values as $15 \leq x_1 \leq 30$, $50 \leq x_2 \leq 80$, $10 \leq x_3 \leq 40$ and $0.5 \leq x_3 \leq 2$.

The Artificial Bee Colony (ABC) algorithm utilizes a swarm size of 200, with 50 % of the swarm size allocated to employed bees and the remaining 50 % to onlooker bees. Each cycle involves 1 scout bee, with a total of 1000 cycles executed over 300 iterations and a limit set at 50. The Ant Colony Optimization (ACO) method employs a sample size of 200, an intensification factor of 0.5, and a deviation distance ratio of 1, all executed over 300 iterations. The Firefly Algorithm (FA) runs with 200 fireflies, utilizing a light absorption coefficient of 1, an initial randomness factor of 0.9, and subsequent randomness factor adjustments of 0.91 with a reduction rate of 0.75 over 300 iterations. The Differential Evolution (DE) algorithm operates with a population size of 200, employing a scaling factor ranging from 0.2 to 0.8 and a crossover probability of 0.9 across 300 iterations. The Teaching-Learning Based Optimization (TLBO) method is configured with a population size of 200 over 300 iterations, while the Dynamic Teaching-Based Optimization (DTBO) shares the same parameters of a population size of 200 over 300 iterations. Each algorithm's distinctive parameters aim to optimize performance across their respective problem domains, reflecting a range of approaches from swarm intelligence to evolutionary and metaheuristic methodologies.

The results from single objective optimization presented in the Table 1 reveal that the DTBO algorithm demonstrates superior performance compared to other algorithms in terms of achieving output with greater accuracy and lesser standard deviation (SD) values. This superiority is further affirmed by the box plots shown in the Fig. 2, which illustrate the consistent delivery of optimal solutions with minimal variability by the DTBO algorithm. These findings underscore DTBO's efficacy in tackling optimization challenges by consistently producing results that are both precise and stable, making it a robust choice for various optimization tasks. The boxplots depicted in Fig. 2 clearly demonstrate that the optimal solutions obtained through the DTBO algorithm exhibit the least variability compared to other algorithms. Furthermore, the convergence diagrams illustrated in Fig. 3 reinforce that the DTBO algorithm requires minimal computational effort in terms of both time and speed. Notably, the convergence patterns reveal that the DTBO algorithm achieves optimum solutions for the considered outputs within a remarkably efficient range of just 4 to 10 iterations (Table 2).

Fig. 4 illustrates the relationship between Material Removal Rate (MRR) and average power. The scatter plot plotted with the help of DTBO vividly showcases a concentration of data points at higher average power levels, indicative of an optimal range where MRR is maximized. This clustering underscores the significance of selecting appropriate average power settings to achieve optimal material removal rates effectively. Similar trends appear concerning pulse frequency, as depicted in the scatter plot. Here, an upward trajectory is observed, with MRR increasing alongside pulse frequency. The dominance of data points at higher pulse frequencies emphasizes the efficacy of this parameter in enhancing material removal rates. In the case of scanning speed, the scatter plot reveals a different pattern as compared to average power and pulse frequency characterized by a concentration of data points between the highest and lowest values tested. This clustering suggests that the optimal scanning speed lies within this range, emphasizing the importance of carefully selecting scanning parameters to optimize material removal efficiency. Similarly, the scatter plot elucidates the optimal range for gas pressure, situated between the highest and lowest values examined. This observation underscores the criticality of fine-tuning gas pressure settings to achieve optimal material removal rates.

The Fig. 5 illustrates the significance of laser parameters on the average texture width (ATW). The plot reveals a clustering of data points at lower average power values, indicating an optimal range where ATW is minimized. This concentration highlights that the lower value of average power remain appropriate to achieve minimum ATW. Similar findings are evident concerning pulse frequency and ATW. Here, a noticeable dip in ATW occurs at lower pulse frequencies, accompanied by a higher density of data points. This correlation suggests that lower pulse frequencies are conducive for minimizing ATW. Regarding scanning speed and material removal rate (MRR), the plot illustrates that minimum ATW coincides with lower scanning speed values and the

Table 1
Single-objective optimization for MRR.

Method	Mean	SD	Avg. Power (W)	Pulse Frequency (KHz)	Scanning Speed (mm/s)	Gas Pressure (kgf/cm^2)	MRR (mg/s)
ABC	0.006874	2.099E-05	22.2091	79.846	16.737	1.361	0.0069
ACO	0.007144	0.0001092	30	50	26.333	1.338	0.0072
FA	0.007353	2.09E-05	30	61.256	26.677	1.417	0.0074
DE	0.007837	1.66E-05	30	80	35.513	2	0.0078
TLBO	0.00798	4.616E-05	30	80	32.267	2	0.0080
DTBO	0.00871	2.832E-05	30	80	26.333	1.338	0.0087

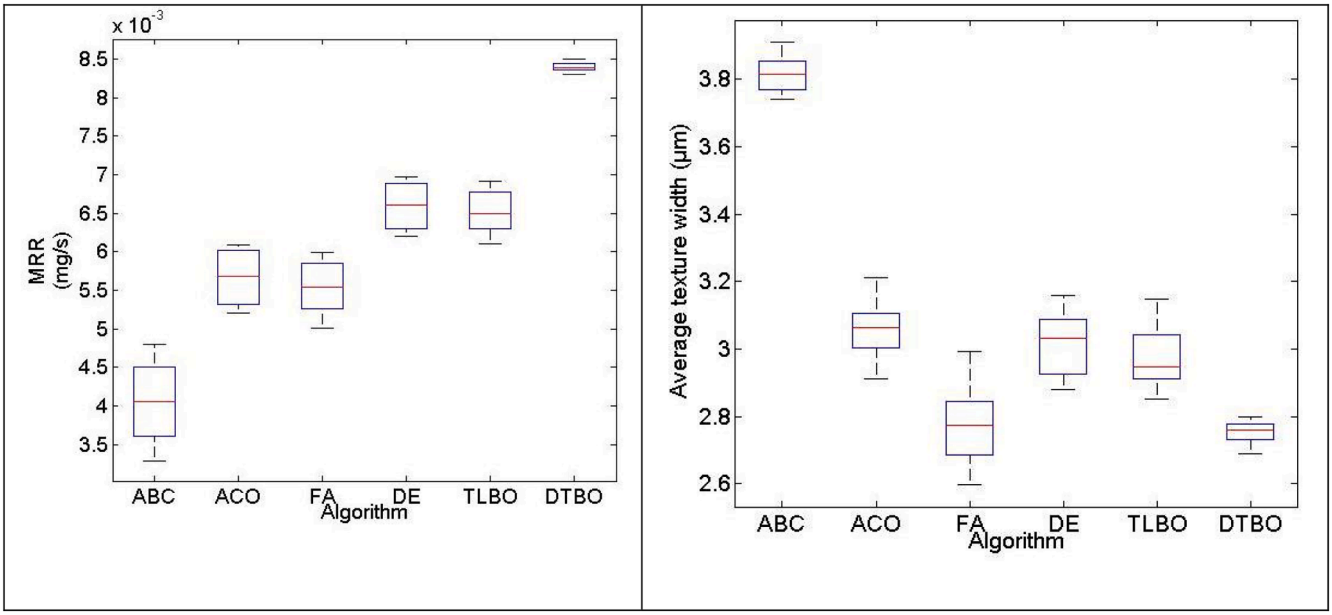

Fig. 2. Boxplots for the considered metaheuristic algorithms.

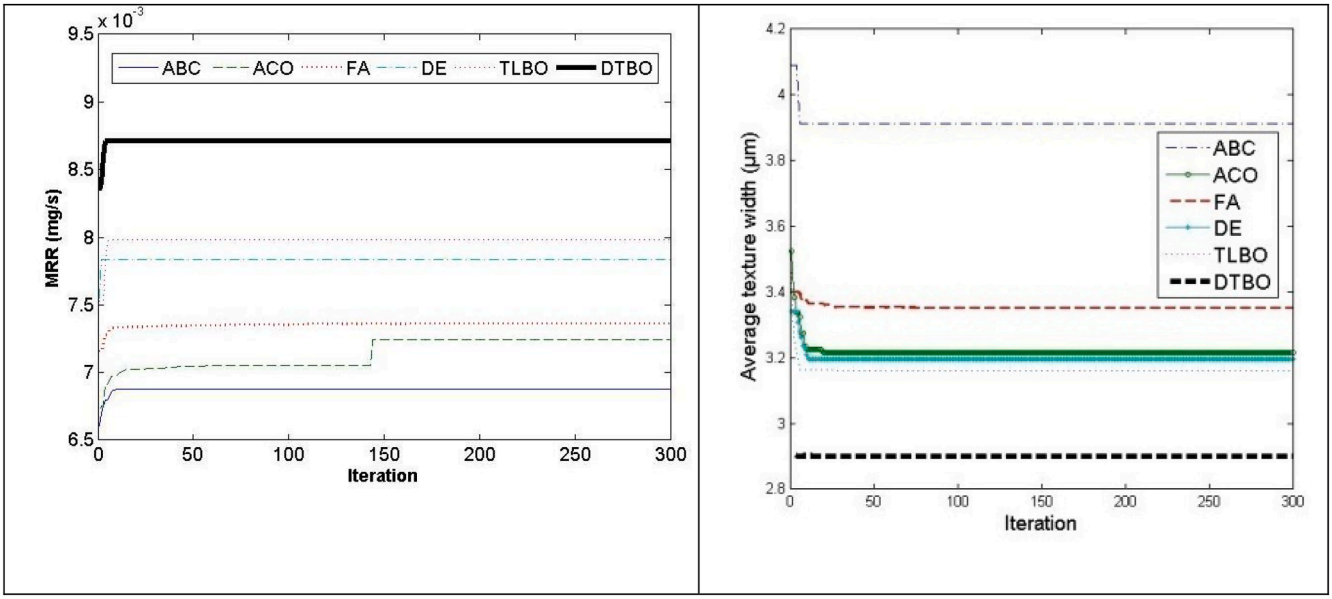

Fig. 3. Convergence diagrams for the metaheuristic algorithms.

Table 2
Single-objective optimization for ATW.

Method	Mean	SD	Avg. Power (W)	Pulse Frequency (KHz)	Scanning Speed (mm/s)	Gas Pressure (kgf/cm^2)	ATW (μm)
ABC	3.915	0.021	21.085	66.074	11.778	2	3.913
ACO	3.221	0.025	19.455	80	40	2	3.217
FA	3.353	0.007	18.267	80	14.366	2	3.352
DE	3.198	0.024	19.060	80	40	2	3.194
TLBO	3.160	0.019	18.294	80	40	2	3.158
DTBO	2.901	0.002	15.584	50	10	2	2.900

concentration of data points are maximum at lower values of scanning speed. Conversely, the influence of gas pressure on ATW appears negligible, as evidenced by the absence of a discernible trend in the plot. This observation suggests that variations in gas pressure do not exert a significant effect on ATW compared to other laser parameters.

5. Hypothesis testing

To measure the statistical importance of the outcomes attained from the above mentioned optimization methods, a hypothesis testing approach using a paired *t*-test is employed [33]. The paired *t*-test

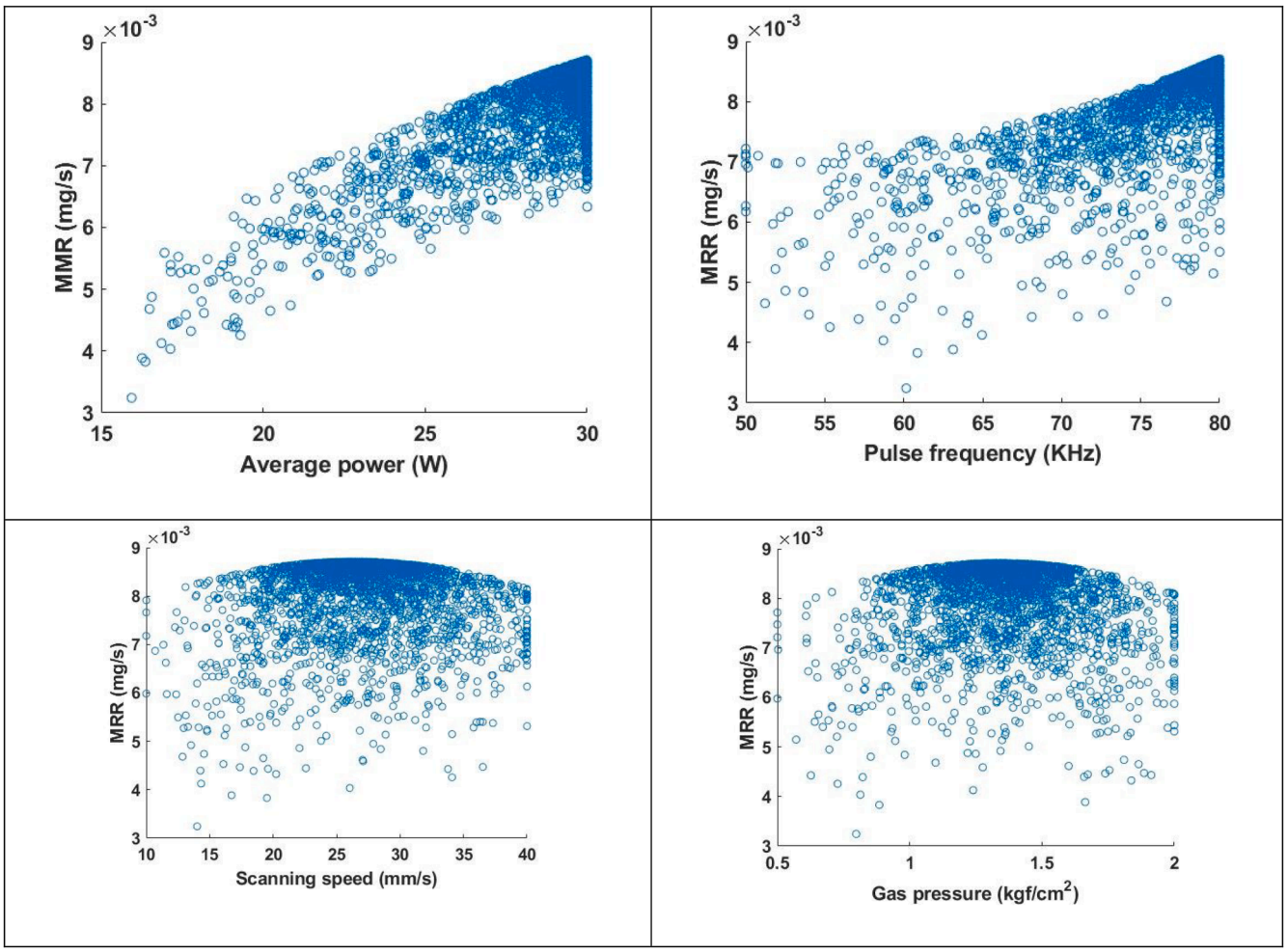

Fig. 4. Effects of LBM process parameters on MRR based on DTBO.

represents a statistical method employed to understand the average difference amongst two populations is statistically significant or not and also provides insights into whether there exist a meaningful difference in the means of two sets of samples assuming their distributions are normal. In this study, the paired *t*-test is conducted to assess the exclusivity of the DTBO algorithm and to identify if there are significant differences in optimization performance among several algorithms utilized in this research. The paired *t*-test is carried out based on the subsequent hypotheses: the null hypothesis (equal population means) and the alternative hypothesis (unequal population means). The output of the *t*-test is presented in Table 3. The population means specified in the hypotheses represent the average values of output obtained subsequently 300 repetitions for respective algorithm. The null hypothesis are not taken into consideration as the absolute values of outputs are much substantial than the imperative *t*-test value of 0.05. These *t*-test marks the uniqueness of the DTBO algorithm compared to the other algorithms examined, particularly in achieving optimal results for single and multi-objective optimization tasks, respectively.

To enhance the output responses effectively, it is highly advisable to optimize both Material Removal Rate (MRR) and Average Tool Wear (ATW) concurrently, aiming to discover an optimal combination of input parameters. In practical machining scenarios, it is impractical for operators to adjust parameters at various operating levels within a single setup. Therefore, a multi-objective optimization model has been formulated to address both MRR and ATW simultaneously, leveraging the selected algorithms for solution generation and evaluation.

$$Z = -w_1 Y(MRR)/MRR_{\max} + w_2 Y(ATW)/ATW_{\min} \quad (14)$$

where, Z is the multi-objective function. w_1, w_2 represents allocated weights. MRR_{max} and ATW_{min} the higher MRR and lower ATW values achieved through single-objective optimization. In the multi-objective optimization model, weights are assigned as $w_1 + w_2 = 1$, with equal weighting given to both MRR and ATW. The solutions derived from this model are précised in Table 4. It is obvious from the table that the DTBO algorithm consistently beats the other five algorithms in respect of both the accuracy and consistency of optimal solutions obtained. Specifically, Table 4 highlights that DTBO achieves a higher MRR by 35.7 %, 20 %, 11.9 %, 54.7 %, and 33.3 % compared to ABC, ACO, FA, DE, and TLBO, respectively. Simultaneously, DTBO also achieves a lower ATW by 13.6 %, 14.8 %, 3.02 %, 15.9 %, and 16.1 % compared to the same algorithms. These results underscore DTBO's superior performance in achieving improved MRR values and reduced ATW values across the considered optimization algorithms.

During multi-objective optimization of both MRR and ATW with DTBO algorithm, initially the MRR is maximized and the set of all the points generated during each iteration are collected. A clear convergence is observed towards maximum value of MRR. Then in the second run, ATW is independently minimized using the DTBO algorithm to achieve similar set of points. Minimum ATW is achieved as per the trend observed in the scatter plots. Then a Pareto front (a set of non-dominated solutions) is developed for ATW against MRR combining the two data sets collectively. The Pareto front concurrently has the minimum ATW and maximum MRR values.

Table 5 presents a set of 30 such solution sets and the entire set of Pareto optimal solution is plotted in Fig. 6. For maximum MRR of

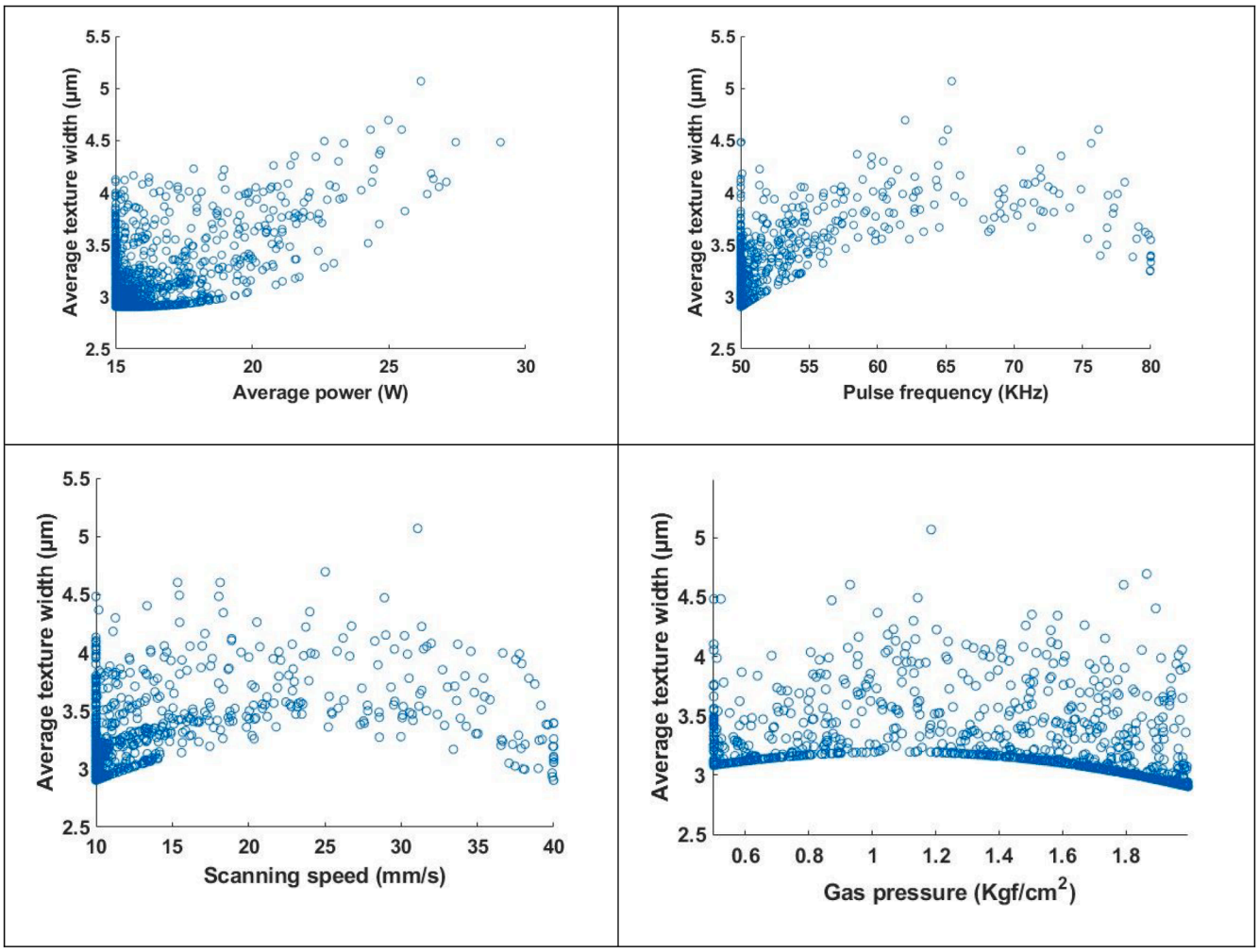

Fig. 5. Effects of LBM process parameters on Average texture width based on DTBO.

Table 3
Results of two tailed paired *t*-test corresponding to DTBO algorithm.

Optimization	Responses	ABC	ACO	FA	DE	TLBO
Single-objective	MRR	263.43	1467.10	770.61	235.56	534.36
	ATW	−857.06	−217.53	−1067.5	−271.89	−239.78
Multi-objective	*Z*	−566.32	−664.89	−650.51	−1057.45	−150.92

Table 4
Results of multi-objective optimization (w_1=0.5,w_2=0.5).

Method	Response	Optimal Output	*Z*	Mean	SD	Avg. Power (W)	Pulse Frequency (KHz)	Scanning Speed (mm/s)	Gas Pressure (kgf/cm^2)
ABC	MRR	0.0027	0.6811	0.726	0.005	15.13	69.15	10.88	2
	ATW	3.167							
ACO	MRR	0.0036	0.668	0.669	0.003	18.97	51.79	40	2
	ATW	3.122							
FA	MRR	0.0037	0.724	0.726	0.005	18.65	58.76	39.24	2
	ATW	3.556							
DE	MRR	0.0019	0.774	0.775	0.004	15	50	10	0.5
	ATW	3.083							
TLBO	MRR	0.0028	0.0602	0.604	0.009	16.56	51.23	11.33	2
	ATW	3.075							
DTBO	MRR	0.0069	−0.0106	−0.0103	0.001	23.74	80	40	1.53
	ATW	3.835							

0.007474 mg/s and maximum ATW of 4.242 μm, the parametric combination are average Power = 23.593 W, pulse frequency = 80 KHz, scanning speed = 28.366 mm/s and gas pressure = 1.295 kgf/cm^2. For minimum MRR of 0.006908 mg/s and minimum ATW of 3.834 μm, the parametric combination are average Power = 23.746 W, pulse frequency = 80 KHz, scanning speed = 40 mm/s and gas pressure = 1.532

Table 5
A complete set of non-dominated solutions.

Sl.No	MRR (mg/s)	ATW (μm)	Avg. Power (W)	Pulse Frequency (KHz)	Scanning Speed (mm/s)	Gas Pressure (kgf/cm^2)
1	0.007225	4.153405	23.40477	80	17.85713	1.276042
2	0.007474	4.242695	23.59391	80	28.36611	1.295603
3	0.007474	4.242695	23.59391	80	28.36611	1.295603
4	0.007501	4.224623	24.1741	80	30.35222	1.555155
5	0.007417	4.162234	24.05168	80	33.20843	1.485786
6	0.007118	3.973373	24.06547	80	37.315	1.620703
7	0.006954	3.867546	24.24006	80	40	1.624056
8	0.006954	3.867546	24.24006	80	40	1.624056
9	0.006964	3.869615	24.16301	80	40	1.590177
10	0.00693	3.849398	24.00787	80	40	1.589908
11	0.006865	3.811506	23.68063	80	39.99972	1.579207
12	0.006865	3.811506	23.68063	80	39.99972	1.579207
13	0.00687	3.813686	23.62028	80	39.99989	1.550209
14	0.006921	3.842332	23.77798	80	39.99995	1.521777
15	0.00692	3.841239	23.77135	80	40	1.522609
16	0.00692	3.841239	23.77135	80	40	1.522609
17	0.00692	3.841239	23.77135	80	40	1.522609
18	0.006911	3.83617	23.75344	80	40	1.531729
19	0.006908	3.834912	23.74601	80	40	1.532768
20	0.006909	3.835162	23.74641	80	40	1.532131
21	0.006908	3.834875	23.744	80	40	1.532075
22	0.006908	3.834875	23.744	80	40	1.532075
23	0.006908	3.834845	23.74365	80	40	1.532033
24	0.006908	3.834827	23.74341	80	40	1.531992
25	0.006908	3.834858	23.74285	80	40	1.531668
26	0.006908	3.834858	23.74285	80	40	1.531668
27	0.006908	3.834859	23.74265	80	40	1.531581
28	0.006908	3.834866	23.74264	80	40	1.531557
29	0.006908	3.834882	23.7427	80	40	1.531531
30	0.006909	3.834965	23.74309	80	40	1.531422

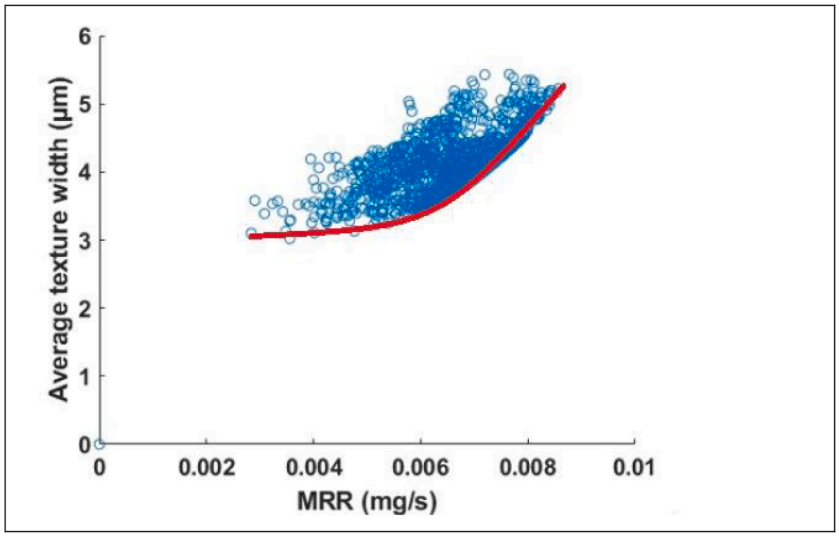

Fig. 6. A complete set of Pareto points.

kgf/cm^2. The Pareto front, suggests an intermediate settings of responses which would direct the operator of the machine to choose optimal parametric mix of process parameters for the considered machining process.

6. Conclusion

The research thoroughly examined the efficacy of the LBM process in generating textures on Ti-6Al-4V, with a particular emphasis on optimizing critical parameters such as average power, pulse frequency, scanning speed, and gas pressure. The DTBO algorithm was employed for both single and multi-objective optimizations, and its effectiveness was rigorously assessed against five other metaheuristic algorithms. The results indicated that DTBO achieves a higher MRR by 35.7 %, 20 %, 11.9 %, 54.7 %, and 33.3 % compared to ABC, ACO, FA, DE, and TLBO, respectively. Simultaneously, DTBO also achieves a lower ATW by 13.6 %, 14.8 %, 3.02 %, 15.9 %, and 16.1 % compared to the same algorithms. The DTBO algorithm consistently surpassed its competitors in terms of accuracy in identifying optimal solutions with minimal variability and reduced computational demands. This advantage was clearly illustrated through the use of box plots and convergence diagrams, which highlighted the robustness of the DTBO algorithm. Moreover, statistical evaluations, including paired *t*-tests, validated the distinctiveness and reliability of the DTBO algorithm compared to the other algorithms tested. This underscores its effectiveness in optimizing the parameters of the laser beam texturing process. Looking forward, future

investigations could assess the applicability of the DTBO algorithm in combination with both traditional and non-traditional machining processes. Additionally, exploring the effects of varying weights assigned to different responses in multi-objective optimization contexts could further improve the algorithm's performance and expand its practical applications.

CRediT authorship contribution statement

Ishwer Shivakoti: Writing – original draft, Visualization, Resources, Conceptualization. **Sunny Diyaley:** Validation, Software, Investigation, Formal analysis. **Partha Protim Das:** Writing – original draft, Validation, Project administration, Funding acquisition. **Abhijit Bhowmik:** Writing – review & editing, Supervision, Methodology, Data curation. **A. Johnson Santhosh:** Writing – review & editing, Supervision, Methodology, Data curation.

Declaration of competing interest

The authors declare that they have no known competing financial interests or personal relationships that could have appeared to influence the work reported in this paper.

Data availability

Data will be made available on request.

References

[1] I. Shivakoti, G. Kibria, R. Cep, B.B. Pradhan, A. Sharma, Laser surface texturing for biomedical applications: a review, Coatings 11 (2) (2021) 124.

[2] Y. Demircan, S. Gemici, A &Sert, Laser surface texturing and techniques to improve the tribological properties of materials, Open J. Nano 6 (2) (2021) 41–58.

[3] Z. Liu, T. Niu, Y. Lei, Y. Luo, Metal surface wettability modification by nanosecond laser surface texturing: a review, Biosurf. Biotribol. 8 (2) (2022) 95–120.

[4] I. Evangelista, D. Wencel, S. Beguin, N. Zhang, M.D. Gilchrist, Influence of surface texturing on the dry tribological properties of polymers in medical devices, Polymers. (Basel) 15 (13) (2023) 2858.

[5] A. Riveiro, A.L. Maçon, J. del Val, R. Comesaña, J. Pou, Laser surface texturing of polymers for biomedical applications, Front. Phys. 6 (2018) 16.

[6] J. Xu, M. Ji, L. Li, Y. Wu, Q. Yu, M. Chen, Improving wettability, antibacterial and tribologicalbehaviors of zirconia ceramics through surface texturing, Ceram. Int. 48 (3) (2022) 3702–3710.

[7] M. Ji, J. Xu, M. Chen, M. El Mansori, Enhanced hydrophilicity and tribologicalbehavior of dental zirconia ceramics based on picosecond laser surface texturing, Ceram. Int. 46 (6) (2020) 7161–7169.

[8] W. Tong, D. Xiong, Direct laser texturing technique for metal surfaces to achieve superhydrophobicity, Mater. Today Phys. 23 (2022) 100651.

[9] S. Yuan, N. Lin, W. Wang, H. Zhang, Z. Liu, Y. Yu, Y. Wu, Correlation between surface textural parameter and tribological behaviour of four metal materials with laser surface texturing (LST), Appl. Surf. Sci. 583 (2022) 152410.

[10] I. Shivakoti, K. Kalita, G. Kibria, A. Sharma, B.B. Pradhan, R.K. Ghadai, Parametric analysis and multi response optimization of laser surface texturing of titanium super alloy, J. Braz. Soc. Mech. Sci. Eng. 43 (2021) 1–15.

[11] D.L. Soni, J. Jagadish, Selection of nature-inspired surface texture pattern for machining applications: an integrated approach, in: Proceedings of the *AIP Conference Proceedings* (Vol. 3006, No. 1), AIP Publishing, 2023.

[12] S. Ürgün, H. Yiğit, S. Fidan, T. Sınmazçelik, T &Canel, Optimization of laser-texturing process parameters of Ti6Al4V alloys using metaheuristic algorithms, Proc. Inst. Mech. Eng. Part E J. Process Mech. Eng. (2024) 09544089241241129.

[13] J.W. SUN, P. Yi, H.Y. JIA, X.S. YANG, Y.P. ZHAN, K. Gao, Using a hybrid neural network to predict the surface morphology of laser surface textured Ni-coated MoS2 40Cr alloy steel, Lasers Eng. 56 (2023) *(Old City Publishing)*.

[14] T. Steege, G. Bernard, P. Darm, T. Kunze, A.F. Lasagni, Prediction of surface roughness in functional laser surface texturing utilizing machine learning, Photonics 10 (4) (2023) 361. VolNo.

[15] R. Thomas, E. Westphal, G. Schnell, H. Seitz, Machine learning classification of self-organized surface structures in ultrashort-pulse laser processing based on light microscopic images, Micromachines. (Basel) 15 (4) (2024) 491.

[16] Z. Zhang, Z. Yang, Z. Zhao, Y. Liu, C. Wang, W. Xu, Multimodal deep-learning framework for accurate prediction of wettability evolution of laser-textured surfaces, ACS Appl. Mater. Interfaces 15 (7) (2023) 10261–10272.

[17] S. Diyaley, S. Chakraborty, Optimization of multi-pass face milling parameters using metaheuristic algorithms, FactaUniv. Ser. Mech. Eng. 17 (3) (2019) 365–383.

[18] K. Vijayakumar, G. Prabhaharan, P. Asokan, R. Saravanan, Optimization of multi-pass turning operations using ant colony system, Int. J. Mach. Tools Manuf. 43 (15) (2003) 1633–1639.

[19] M.F.F. Ab Rashid, N.M.Z. Nik Mohamed, A.N. Mohd Rose, S.A. Che Ghani, W.S. W Harun, Implementation of ant colony optimization algorithm to minimize cost of turning process, Appl. Mech. Mater. 695 (2015) 558–561.

[20] S. Bharathi Raja, N. Baskar, Particle swarm optimization technique for determining optimal machining parameters of different work piece materials in turning operation, Int. J. Adv. Manuf. Technol. 54 (2011) 445–463.

[21] P.K. Shrivastava, A.K. Pandey, Optimization of machining parameter during the laser cutting of Inconel-718 sheet using regression analysis based particle swarm optimization method, Mater. Today Proc. 5 (11) (2018) 24167–24176.

[22] D. Pramanik, N. Roy, A.S. Kuar, S. Sarkar, S. Mitra, Experimental investigation of sawing approach of low power fiber laser cutting of titanium alloy using particle swarm optimization technique, Optics Laser Technol. 147 (2022) 107613.

[23] Y. Wang, Z. Cai, Q. Zhang, Differential evolution with composite trial vector generation strategies and control parameters, IEEE Trans. Evol. Comput. 15 (1) (2011) 55–66.

[24] R. Storn, K. Price, Differential evolution–a simple and efficient heuristic for global optimization over continuous spaces, J. Glob. Optim. 11 (1997) 341–359.

[25] G.D. Gautam, D.R. Mishra, Firefly algorithm based optimization of kerf quality characteristics in pulsed Nd: YAG laser cutting of basalt fiber reinforced composite, Compos. Part B Eng. 176 (2019) 107340.

[26] B. Narayana Reddy, P. Hema, Y. Prasanth Reddy, G. Padmanabhan, Experimental investigation on laser beam welded joints of dissimilar metals and optimization of process parameters using firefly algorithm, in: Proceedings of the *Advances in Applied Mechanical Engineering: Select Proceedings of ICAMER 2019*, Springer Singapore, 2020, pp. 823–830.

[27] N. Singh, P.S. Bharti, Multi-Objective parametric optimization during micro-EDM drilling of Ti-6Al-4V using teaching learning Based optimization algorithm, Mater. Today Proc. 62 (2022) 262–269.

[28] D. Pramanik, T. Singh, N. Roy, R. Biswas, A.S. Kuar, S. Sarkar, S. Mitra, Analysis of performance characteristics with artificial intelligence based TLBO technique for laser drilling of Monel superalloy, Optics Laser Technol. 164 (2023) 109554.

[29] M.K. Das, K. Kumar, T.K. Barman, P. Sahoo, Application of artificial bee colony algorithm for optimization of MRR and surface roughness in EDM of EN31 tool steel, Procedia Mater. Sci. 6 (2014) 741–751.

[30] P.J. Pawar, M.Y. Khalkar, Multi-objective optimization of wire-electric discharge machining process using multi-objective artificial bee colony algorithm, in: Proceedings of the *Advanced Engineering Optimization Through Intelligent Techniques: Select Proceedings of AEOTIT 2018*, Springer Singapore, 2020, pp. 39–46.

[31] M. Dehghani, E. Trojovská, P. Trojovský, A new human-based metaheuristic algorithm for solving optimization problems on the base of simulation of driving training process, Sci. Rep. 12 (1) (2022) 9924.

[32] I. Shivakoti, K. Kalita, G. Kibria, A. Sharma, B.B. Pradhan, R.K. Ghadai, Parametric analysis and multi response optimization of laser surface texturing of titanium super alloy, J. Braz. Soc. Mech. Sci. Eng. 43 (2021) 1–15.

[33] P.K. Mahto, P.P. Das, S. Diyaley, B. Kundu, Parametric optimization of solar air heaters with dimples on absorber plates using metaheuristic approaches, Appl. Therm. Eng. 242 (2024) 122537.